Up-Regulation of MiR-330-5p is Associated with the Advanced Clinical Stage of Hepatocellular Carcinoma

Hong-Yu Wei
Guangxi Medical University
He-Qing Huang
Guangxi Medical University
Gang Chen
Guangxi Medical University
Jie-Zhuang Huang
Guangxi Medical University
Yi-Wu Dang
Guangxi Medical University
Zhi-Guang Huang
Guangxi Medical University
Li-Min Liu
Guangxi Medical University
wei hou (houwei@gxmu.edu.cn)
Guangxi Medical University

Research

Keywords: Hepatocellular carcinoma, hsa-miR-330-5p, in house RT-qPCR, standard mean difference (SMD), summary receiver operating characteristic curve (sROC)

Posted Date: April 12th, 2021

DOI: https://doi.org/10.21203/rs.3.rs-384872/v1

Abstract

Purpose: A opposite expression levels and roles of miR-330-5p in hepatocellular carcinoma (HCC) have been reported in previous studies, so the clinicopathological implications and the prospective molecular mechanism of miR-330-5p in HCC require elaboration.

Materials and methods: To examine the mRNA expression profile of hsa-miR-330-5p in HCC, a in-house RT-qPCR was performed, and the expression data was extracted from sequencing data and gene microarrays from the datasets of The Cancer Genome Atlas (TCGA), Gene Expression Omnibus (GEO), ONCOMINE, ArrayExpress, and Sequence Read Archive (SRA). To have an overview of the clinical value of miR-330-5p, all possible data were integrated to calculate the standard mean difference (SMD) and area under the curve (AUC) from summary receiver operating characteristic curve (sROC). The target genes of miR-330-5p were also predicted and the relative signaling pathways were investigated by Gene Ontology (GO) and Kyoto Encyclopedia of Genes and Genomes (KEGG) analyses.

Results: According to the integrative analysis, the expression value of miR-330-5p in HCC was higher than in non-tumor tissue (SMD=0.47, 95CI%=0.31-0.63), and high expression of miR-330-5p was related with advanced HCC stage (SMD=0.27, 95CI%=0.08-0.46), poor differentiation (SMD=0.39, 95CI%=0.21-0.58) and poor prognosis (HR=1.91, Log-rank P=0.014). GLUD1, GOT1 and GLS2 were highly likely to be targeted by miR-330-5p, and the progression and prognosis of HCC might be influenced via the miR-330-5p–GLUD1/GOT1/GLS2 axis.

Conclusion: The result showed a high-expressed level of miR-330-5p was in the HCC tissue compared with non-tumor tissue, and the overexpression of miR-330-5p indicated poor progression and prognosis in HCC.

Introduction

MicroRNAs (miRNAs) are short, endogenous, single-strand RNA molecules regulating gene expression. They particularly inhibit protein translation or promote mRNA degradation by interacting with the 3'-untranslated region (3'-UTR) of targets [12–15]. Many studies have documented that deregulation of miRNA is associated with the progression and development of malignant tumors [16–18]. MiR-330-5p, a type of miRNA, has been verified to play an important role in the cell growth, migration, and infiltration of some malignancies, such as glioblastoma, cutaneous malignant melanoma, pancreatic cancer, lung cancer, and ovarian cancer [19–23]. However, opposite expression levels and roles of miR-330-5p in HCC have been reported in studies from different groups. Downregulation of miR-330-5p has been observed in the cancer cells and exosomes of HCC [24, 25]; contradictorily, overexpression of miR-330-5p has also been found in HCC tissues [26–28]. The molecular mechanism of miR-330-5p in HCC remains largely unclarified, as only a few targets have been documented thus far, including inhibitor of growth 4 (ING4) [28], Sprouty2 (SPRY2) [27], organic cation transporter-1 (OCT1) [26], talin-1 (TLN1) [29], and checkpoint kinase 1 (CHEK1) [24]. The clinicopathological implications and the prospective molecular mechanism of miR-330-5p in

HCC require elaboration. In the present study, we carried out a comprehensive investigation with various detecting assays to inspect the clinicopathological value and probable molecular mechanism of miR-330-5p in HCC.

Materials And Methods

2.1 Expression of miR-330-5p in HCC tissues

2.1.1 MiR-330-5p expression in HCC detected by in-house RT-qPCR

To examine the clinicopathological implications of miR-330-5p in HCC, 26 pairs of HCC and non-HCC liver tissues were collected in the Department of Pathology of the First Affiliated Hospital of Guangxi Medical University (Nanning, Guangxi, People's Republic of China). The samples were randomly collected from untreated surgically resected patients. All the experimental protocols were approved by the Ethics Committee of the First Affiliated Hospital of Guangxi Medical University, and both the clinician and the patient signed the consent form for the use of samples for the research. Total RNA was isolated and then subjected to cDNA synthesis with TaqMan Reagent as recommended by the manufacturer's instructions. One μg RNA was reversed into 20 μl complementary DNA (cDNA), and RT-qPCR was performed using miScript SYBR-Green PCR kit on a 7900HT PCR system (Applied Biosystems; Thermo Fisher Scientific, Inc., Waltham, MA, USA). The primer was provided by Applied Biosystems (Thermo Fisher Scientific, Inc.) with the sequence GCAAAGCACACGGCCUGCAGAGA (cat. no. 4427975-002230). The relative expression level of miR-330-5p was calculated in comparison to the combination of RNU6B and RNU48 previously reported [30–32].

2.1.2 MiR-330-5p expression in HCC based on miRNA-microarray and miRNA-sequencing data

Since the in-house RT-qPCR detection was carried out based on a small sample size with 52 paired HCC cases, we further mined data from miRNA-microarray and miRNA-sequencing to evaluate the miR-330-5p expression in HCC with various detecting methods. Datasets including The Gene Expression Omnibus (GEO), ArrayExpress, Sequence Read Archive (SRA), and peer reviewed publications were used to screen relevant miRNA-microarray and miRNA-sequencing data involving miR-330-5p expression in HCC [33–35]. The keywords "hepatocellular carcinoma" and "HCC" were searched in the above datasets. The inclusion criteria were set as: 1) human samples; 2) miR-330-5p expression data being available; 3) non-cancerous liver controls being sufficient. Finally, 22 miRNA-microarrays from GEO and one from ArrayExpress that met the requirements were recruited. The expression of miR-330-5p in HCC and adjacent liver control tissues was also obtained from TCGA miRNA-sequencing (Supplementary Figure 1) [36, 37]. The violin charts were drawn using ggplot2 packages for each dataset to visualize the different expressions of miR-330-5p. Box plots were also inserted to reflect the average value and quartile. Student's t-test was used to evaluate the different levels of miR-330-5p between groups.

2.1.3 Validation of miR-330-5p expression in HCC via integrated analysis

The results of RT-qPCR, miRNA-microarray, and miRNA-sequencing were merged to show the overall expression level of miR-330-5p in HCC. The standard mean difference (SMD) and a 95% confidence interval (95%CI) were determined using meta R packages and STATA 12.0. A random effect model or fixed-effect model was chosen according to the I^2 test and Chi-square test; high heterogeneity existed if I^2>50% or P<0.05. Sensibility analysis was conducted to investigate the highly heterogeneous datasets. A funnel plot was also drawn to detect publication bias. The ROC curves were performed for each set, and the area under curves (AUCs) were calculated using SPSS 22.0 to access the predictive capacity of miR-330-5p for HCC. Next, sROC was performed for all datasets via STATA 12.0. The summarized AUC was calculated along with the sensitivity and specificity.

2.1.4 Analysis of the clinicopathological role of miR-330-5p in HCC

Information on related clinicopathological parameters, such as gender, age, tumor grading, tumor-regional lymph node-metastasis (TNM) staging, alcohol addiction, HBV infection, HCV infection, and albumin value was extracted to analyze the relationships between miR-330-5p and development of HCC based on miRNA-sequencing and in-house RT-qPCR data. The prognostic data of miR-330-5p was extracted from available datasets to perform an integrated prognostic analysis. The result was visualized by K-M curves, and the single hazard ratio (HR) and the summarized HR were evaluated.

2.2 Screening of overlapping target genes

2.2.1 Differently expressed genes (DEGs) of HCC

To obtain the differentially expressed genes (DEGs) in HCC tissues for intersection with the predicted target genes of miR-330-5p and narrow the range of potential target genes of miR-330-5p, we obtained raw data from 63 high-throughput RNA-sequencing and microarrays (data not shown). Eventually, a total of 11 different detection platforms were included. The DEGs of RNA-sequencing data were calculated using Limma Voom and microarrays using Limma (logfc>1, adj P<0.05). After removing the batch effect of different platforms, 1,478 over-expressed genes appearing over eight times in 11 platforms were collected for subsequent use.

2.2.2 Prediction of miR-330-5p target genes

MiRWalk 2.0 was used for miRNA target prediction [(38)]. The target genes of miR-330-5p were predicted by 12 prediction software programs from MiRWalk. The target genes of miR-330-5p were intersected with the above 1,478 DEGs of HCC tissues. The overlapping genes were regarded as the most likely potential targets of miR-330-5p in HCC.

2.2.3 Signaling pathway enrichment analyses of miR-330-5p potential targets

The ClusterProfiler package was used to provide biofunctional enrichment data required for Gene Ontology (GO) and the Kyoto Encyclopedia of Genes and Genomes (KEGG). The GO items were selected at P<0.05 and FDR<0.05, and the KEGG items were selected at P<0.05. The top 10 signal pathways

enriched by DEGs were listed according to the P value. The results of GO and KEGG analyses were exhibited in a bubble chart and chord chart via the “GO plot” package. The amount of enrichment genes in each term were represented by the size of the bubble, and the P value of each term was shown in gradual color. The genes enriched in the top three pathways were screened to analyze protein-protein interaction (PPI) networks. Protein interactions included direct physical interactions and indirect functional correlations; the interaction pairs in a PPI network were considered with a combined score >0.9 (39-43).

Results

3.1 Expression of miR-330-5p in HCC

3.1.1 Expression of miR-330-5p in HCC based on in-house RT-qPCR and other datasets

MiR-330-5p was markedly over-expressed in HCC tissues assessed by RT-qPCR, which was consistent with data shown by the high-throughput databases of different platforms, including Illumina Human v2 MicroRNA expression beadchip, Applied Biosystems Human MicroRNA Array A v2.0, Agilent-046064 Unrestricted_Human_miRNA_V19.0_Microarray, Affymetrix Multispecies miRNA-2 Array, and Agilent-070156 Human miRNA. Because of the uneven distribution of the results from a single platform, we integrated all the data and found that the SMD was 0.29 [0.05–0.54]. This implied that the expression level of miR-330-5p was predominantly higher in HCC than in non-tumor tissues under a random effect model with 1,315 cases of HCC and 880 control cases (Figure 2A). Sensibility analysis was performed to discover the heterogenous chips (Figure 2C). After removing the high-heterogeneity studies, the SMD rose to 0.47 and the trend of high miR-330-5p expression in HCC was more obvious (Figure 3A). There was no publication bias in our study either before or after removing the high-heterogeneity studies.

The ROCs were used to judge the prospective diagnostic significance of miR-330-5p in each dataset (Figure 4). To further validate whether miR-330-5p could be a predictor of HCC, 25 studies, including the in-house RT-qPCR, were summarized to calculate tp, fp, fn, and tn. The final AUC of SROC was 0.76 [0.72–0.80], the sensitivity was 0.72, and the specificity was 0.69. This showed that miR-330-5p could be considered as a tool for discerning HCC from non-HCC liver tissues.

3.1.2 Clinicopathological role of miR-330-5p based on RNA-sequencing and RT-qPCR data

When looking at the clinical role of miR-330-5p in HCC based on a single cohort, we noted that there were close relations between the miR-330-5p expression and the deterioration of HCC. From the RNA-seq data, when the cases were younger and at more advanced tumor grading and clinical TNM stages, the miR-330-5p expression tended to increase (Table 2). Similar up-regulated trends of miR-330-5p expression were confirmed in our own RT-qPCR data. When a tumor had metastasis or tumor thrombus in the blood vessels, miR-330-5p expression turned to be significantly higher. More importantly, several other high-throughput datasets could be leveraged to display the integrated role of miR-330-5p expression in tumor grading and TNM staging. The TNM stage was divided into advanced stage (stage III–IV) and early stage

(stage I–II). Tumor grading was divided into the poorly-differentiated group (G3–G4) and the well-differentiated group (G1–G2). The expression of miR-330-5p in 165 advanced-stage cases was higher than in 343 early-stage cases (SMD=0.27, 95%CI=0.07–0.47) (Figure 8A). Similarly, the expression of miR-330-5p in 178 cases of poorly differentiated HCC tissues was higher than in 353 cases of well-differentiated HCC (SMD=0.39, 95%CI=0.21–0.58) (Figure 8B). The AUC of the miR-330-5p level for separate clinical stages was 0.88, the sensitivity was 0.67 (0.26–0.92), and the specificity was 0.94 (0.36–1.00). The AUC of miR-330-5p expression to differentiate tumor grades was 0.63, the sensitivity was 0.70 (0.57–0.80) and the specificity was 0.34 (0.16–0.59) (Figure 9A–B).

3.1.3 Prognostic implications of miR-330-5p expression based on RNA-seq data

After screening, since no prognostic data were available in other datasets, the RNA-seq data from TCGA was the only available source to assess the clinical role of miR-330-5p expression in HCC. Both OS and RFS data were extracted and used for prognostic analysis, and cutoff values of K-M curves were set to mean or quartile. The prognostic results were statistically significant in both the mean group and quartile group in the OS group; high expression of miR-330-5p was significantly related to unfavorable HCC prognosis, and the HR of the quartile group (HR=1.91) was higher than that of the mean group (HR=1.5, Figure 10A–B). However, in RFS, the expression of miR-330-5p was not significantly associated with HCC prognosis (Figure 10C–D).

3.2 Potential mechanism of miR-330-5p in HCC

3.2.1 Targets of miR-330-5p in HCC

According to the result of the DEGs and miRWalk2.0, 499 genes overlapping the predicted miRNA target genes and the DEGs were achieved for GO and KEGG pathway analysis and miRNA–mRNA network construction (Figure 11A). MiR-30-5p was over-expressed in HCC, so the low-expressed genes in the DEGs were used to intersect predicted target genes to narrow the possibilities. The target genes appeared at least five times on every predictive platform, and DEGs appeared at least six times among all platforms.

The top 10 items in the biological processes, cell components, and molecular function categories were visualized in bubble charts (Table 4, Figure 11B). In biological processes, these overlapping genes are mainly involved in response to drugs, cholesterol metabolic processes, and positive regulation of gene expression. In cell components, these DEGs were enriched in the extracellular exosome, an integral component of plasma membrane, and external side of plasma membrane. In molecular function, these DEGs had the function of cytoskeletal protein binding, steroid hormone receptor activity, and transcription factor binding. The top 10 KEGG signal pathways were also listed (Table 5), and the chord diagrams were introduced (Figure 12A). The results indicated that these DEGs were mainly enriched in alanine, aspartate, and glutamate metabolism, metabolic pathways, and cancer pathways. The three PPI networks were obtained by STRING (Figure 12B–D). The hub genes in each PPI network were screened out via Cytoscape 3.6.1. The hub genes in the alanine, aspartate, and glutamate metabolism pathways were GLUD1, GOT1, and GLS2. Then, GLUD1, ALDH4A1, and GLS2 were considered as hub genes in the PPI

network of metabolic pathways. In the network of cancer pathways, CDH1, CDKN2A, and IGF1 were screened as hub genes.

Discussion

The expression levels of miR-330-5p in HCC cells and tissues have been documented by several research groups. However, the results have been inconsistent. In this study, combining in-house real time RT-qPCR, miRNA-sequencing, miRNA-microarray, and in-silico integrated analysis, we noted that miR-330-5p levels were apparently upregulated in HCC tissues based on 1,095 cases from multiple research centers. More interestingly, we also pointed out that miR-330-5p may accelerate hepatocarcinogenesis via metabolic pathways, cancer pathways, and the signaling pathways of alanine, aspartate, and glutamate metabolism.

Contradictory miR-330-5p levels have been found in HCC cells and tissues by different groups. Downregulation of miR-330-5p was observed in HCC HepG2, HuH-7, Bel-7402, and SMMC-772 cells, compared to L-02 [24]. Two studies showed that ectopic miR-330-5p had a protective function to suppress the cell growth of HCC in vitro and in vivo. The restoration of miR-330-5p could also suppress the migration, invasion, and angiogenesis capacity of the HCC cells [24, 29]. Hence, the above studies concluded that miR-330-5p may play a proactive role in the HCC process, as the increase of miR-330-5p could slow down or even block HCC development. However, higher expression levels of miR-330-5p have also been detected in HCC tissues and cells by three independent groups [26–28]. Among these three studies, 35 pairs of HCC and non-HCC cases from TCGA were detected by RNA-sequencing and miRNA-microarray [26–28]. More importantly, two groups also verified the oncogenic role of miR-330-5p in HCC through in vitro and in vivo experiments [27, 28]. Overexpression of miR-330-5p by transfection of miRNA mimics could assist the cell proliferation of HCC and the formation of HCC tumors, as well as promote cell infiltration ability [27, 28].

In the previous studies, The insufficient sample size influenced the accuracy of the above incompatible results. To have a comprehensive view of the clinicopathological value of miR-330-5p levels in HCC, the current study combined various detecting methods, including in-house real time RT-qPCR, miRNA-sequencing, miRNA-microarray, and SMD and sROC calculation. The RT-qPCR with the clinical samples showed a significantly higher level of miR-330-5p in 26 cases of HCC, with the relative expression of 7.51, 2.52 folds from the non-cancerous controls. To verify this finding, we mined the data from high-throughput datasets. Upregulation of miR-330-5p levels was consistently noted, as the SMD was 0.3 for 1,095 cases of HCC. With the integration of all available data, the final SMD increased to 0.44, which was comparable to the reports of previous studies [26–28]. Hence, together with previous work, the current findings confirm a marked increase in miR-330-5p expression levels in HCC tissues, compared to non-HCC liver tissues. This upregulation may play an oncogenic function in the tumorigenesis of HCC.

In previous studies, conflicting results existed in the expression of miR-330-5p in HCC tissues. Beyond that, the association between miR-330-5p and the clinical parameters of HCC were contradictory. In the

studies in which miR-330-5p was down-regulated in HCC, the expression value of miR-330-5p was negatively related to the progression parameters of HCC. The higher the TNM stage of HCC, the lower the expression value of miR-330-5p was [24, 29]. However, the expression of miR-330-5p was positively associated with the TNM stage of HCC patients in the studies where miR-330-5p was up-regulated in HCC; in these studies, the higher expression of miR-330-5p was connected with poorer prognosis of HCC patients [26–28]. Although this contradiction existed in multiple studies, the researchers only used their own clinical data, including TNM stage and prognostic data; public data were not used in their studies. This lack of independent cohort verification was likely to be the cause of the contradictory results. In addition, Yu et al. reported that the expression of miR-330-5p in lower migrating HCC exosomes was greater than in higher ones [25].

To obtain a comprehensive conclusion, clinicopathological parameters and prognostic data were collected from TCGA and GEO databases. In the TCGA data, the expression of miR-330-5p had no relationship with the TNM stage. However, there was a positive correlation between miR-330-5p levels and TNM stage in our PCR data. Because the TNM stage information existed in some GEO data, a meta-analysis was computed based on TCGA, GEO, and RT-qPCR data. The result showed that a higher expression of miR-330-5p was correlated with a more advanced TNM stage. Moreover, the AUC of miR-330-5p to differentiate advanced TNM stages from early stages showed that the specificity was 0.94, meaning the expression of miR-330-5p could be considered an indicator for tumor progression. Neither the included GEO data nor our PCR data had prognostic information, so the prognostic analysis of miR-330-5p in HCC was performed based on TCGA data. The results showed that miR-330-5p was closely related to patients' overall survival in HCC, and high expression of miR-330-5p led to poorer prognosis, but the expression of miR-330-5p did not affect patients' RFS. Previously, a relationship between miR-330-5p and RFS of HCC patients had been reported, but the literature used only its own data [27] and no public data. Hence, according to TCGA data and previous studies [27, 28], the overexpression of miR-330-5p could cause poorer overall survival of HCC patients.

The molecular function of miR-330-5p in HCC was still not clear, so we used various bioinformatics platforms to inquire into the putative molecular mechanism of miR-330-5p in HCC. First, the target genes of miR-330-5p were forecasted via miRWalk2.0, and the differential expression genes were calculated via 63 high-throughput RNA-sequencing and microarrays. All of the following operations were based on the intersection genes of the two gene sets. The result of KEGG pathway analysis revealed that miR-330-5p targeted genes might be involved in alanine, aspartate, and glutamate metabolism pathways, metabolic pathways, and pathways in cancer. In the top three pathways, there were two pathways associated with metabolism, particularly in glutamate metabolism. Numerous reports had indicated that the glutamate metabolic pathway was extremely important in the development of cancer. Glutamine can be broken down into glutamate, and glutamate can be further decomposed into α-ketoglutarate to promote the TCA cycle [44–46]. Thus, miR-330-5p may play an essential part in liver cancer; miR-330-5p may affect the occurrence and development of liver cancer by targeting related genes of glutamate metabolism to change the metabolic pathway. To further reveal this phenomenon, the hub genes (GLUD1、GOT1、GLS2)

of alanine, aspartate, and glutamate metabolism pathways were screened. GLUD1, glutamate dehydrogenase 1, converted glutamate to alpha-ketoglutarate to promote the TCA cycle [47]. Glazer et al. found that the expression of GLUD1 in HCC tissues was lower than in non-tumorous liver tissues; combined with our study, we could conclude that targeting of GLUD1 by miR-330-5p led to low expression of GLUD1 in HCC [48]. Similarly, as a glutamate metabolism-related gene, GOT1 (glutamic-oxaloacetic transaminase 1), also called AST1, is an extremely important indicator of liver function and could also convert glutamate to alpha-ketoglutarate [49, 50]. Nwosu et al. reported that the expression of GOT1 was down-regulated in poorly differentiated hepatocellular carcinoma cell lines, and the researchers found that GLUD1 was also down-regulated in HCC cell lines [51]. GLS2 (Glutaminase 2) is located on human chromosome 12, and it mainly encodes glutaminase (GA) which converts glutamine into glutamate in the liver [52]. The expression of GLS2 in HCC was evidentiarily lower than in normal liver cells, and the high expression of GLS2 could suppress the growth of HCC cells [47]. GLS2 could also be regarded as a molecular marker to assess the outcome of HCC patients [53]. These results show that all three hub genes could encode key enzymes in glutamine and glutamate metabolic pathways, and all three genes had low expression in HCC. Therefore, the highly expressed miR-330-5p was highly likely to target these three hub genes to form the regulatory axis of miR-330-5p-GLUD1/GOT1/GLS2.

There were some shortcomings in our study. First, although the three key genes (GLUD1, GOT1, GLS2) were highly likely to be the target genes of miR-330-5p, a dual-luciferase experimental confirmation was still deficient. Second, in vivo and in vitro work must still be conducted to assess the regulatory axis of miR-330-5p–GLUD1/GOT1/GLS2.

Conclusion

Contradictory results had been found in previous studies of miR-330-5p, so a series of integrated analyses were implemented to judge the facticity. The result showed a high-expressed level of miR-330-5p was obvious in the HCC tissue compared with non-tumor tissue, and the overexpression of miR-330-5p indicated poor progression and prognosis in HCC. In addition, GLUD1, GOT1 and GLS2 were highly likely to be targeted by miR-330-5p, and the progression and prognosis of HCC might be influenced via the miR-330-5p–GLUD1/GOT1/GLS2 axis.

Declarations

Ethics approval and consent

All the experimental protocols were approved by the Ethics Committee of the First Affiliated Hospital of Guangxi Medical University.

Consent

Both the clinicians and the patients signed the consent forms for the use of samples for the research.

Availability of data and materials

Our data is availible in the manuscript.

Competing interests

The authors declare that they have no competing interests.

Funding

The study was supported by the funds of Guangxi First-class Discipline Project for Basic medicine Sciences (GXFCDP-BMS-2018), Guangxi First-class Discipline Project for Pharmaceutical Sciences (GXFCDP-PS-2018), Promoting Project of Basic Capacity for Young and Middle-aged University Teachers in Guangxi (2019KY0102), Guangxi Higher Education Undergraduate Teaching Reform Project (2020JGA146), Guangxi Medical University Education and Teaching Reform Project (2019XJGZ04) and Guangxi Educational Science Planning Key Project (2021B167).

Authors' contributions

Hong-Yu Wei, Gang Chen, Yi-Wu Dang, Zhi-Guang Huang, Li-Min Liu and Wei Hou conceived and designed the projects. He-Qing Huang, Jie-Zhuang Huang, Yi-Wu Dang and Zhi-Guang Huang performed the experiments. He-Qing Huang, Jie-Zhuang Huang, Hong-Yu Wei and Gang Chen analyzed the data. He-Qing Huang and Jie-Zhuang Huang wrote the draft. Hong-Yu Wei, Li-Min Liu, Gang Chen and Wei Hou raised the funds. All authors read and approved the final manuscript.

Acknowledgements

We gratefully acknowledge all the public datasets used in the current study: The Cancer Genome Atlas (TCGA), Gene Expression Omnibus (GEO), ONCOMINE, ArrayExpress and Sequence Read Archive (SRA).

References

1. Siegel RL, Miller KD, Jemal A. Cancer statistics, 2020. CA Cancer J Clin. 2020;70(1):7-30.
2. Wang G, Wang Q, Liang N, Xue H, Yang T, Chen X, et al. Oncogenic driver genes and tumor microenvironment determine the type of liver cancer. Cell Death Dis. 2020;11(5):313.
3. Fang C, An J, Bruno A, Cai X, Fan J, Fujimoto J, et al. Consensus recommendations of three-dimensional visualization for diagnosis and management of liver diseases. Hepatol Int. 2020;14(4):437-53.
4. Lau KC, Joshi SS, Gao S, Giles E, Swidinsky K, van Marle G, et al. Oncogenic HBV variants and integration are present in hepatic and lymphoid cells derived from chronic HBV patients. Cancer Lett. 2020;480:39-47.

5. Alexander M, Loomis AK, van der Lei J, Duarte-Salles T, Prieto-Alhambra D, Ansell D, et al. Risks and clinical predictors of cirrhosis and hepatocellular carcinoma diagnoses in adults with diagnosed NAFLD: real-world study of 18 million patients in four European cohorts. BMC Med. 2019;17(1):95.
6. Cheng K, Shi J, Liu Z, Jia Y, Qin Q, Zhang H, et al. A panel of five plasma proteins for the early diagnosis of hepatitis B virus-related hepatocellular carcinoma in individuals at risk. EBioMedicine. 2020;52:102638.
7. Chao J, Zhao S, Sun H. Dedifferentiation of hepatocellular carcinoma: molecular mechanisms and therapeutic implications. Am J Transl Res. 2020;12(5):2099-109.
8. Tang L, Chen R, Xu X. Synthetic lethality: A promising therapeutic strategy for hepatocellular carcinoma. Cancer Lett. 2020;476:120-8.
9. Tao K, Bian Z, Zhang Q, Guo X, Yin C, Wang Y, et al. Machine learning-based genome-wide interrogation of somatic copy number aberrations in circulating tumor DNA for early detection of hepatocellular carcinoma. EBioMedicine. 2020;56:102811.
10. Wen P, Chen SD, Wang JR, Zeng YH. Comparison of Treatment Response and Survival Profiles Between Drug-Eluting Bead Transarterial Chemoembolization and Conventional Transarterial Chemoembolization in Chinese Hepatocellular Carcinoma Patients: A Prospective Cohort Study. Oncol Res. 2019;27(5):583-92.
11. Zhang Z, Weng W, Huang W, Wu B, Zhou Y, Zhang J, et al. A novel molecular-clinicopathologic nomogram to improve prognosis prediction of hepatocellular carcinoma. Aging (Albany NY). 2020;12.
12. Ji L, Lin Z, Wan Z, Xia S, Jiang S, Cen D, et al. miR-486-3p mediates hepatocellular carcinoma sorafenib resistance by targeting FGFR4 and EGFR. Cell Death Dis. 2020;11(4):250.
13. Ashrafizadeh M, Najafi M, Mohammadinejad R, Farkhondeh T, Samarghandian S. Flaming the fight against cancer cells: the role of microRNA-93. Cancer Cell Int. 2020;20:277.
14. Li YF, Dong L, Li Y, Wei WB. A Review of MicroRNA in Uveal Melanoma. Onco Targets Ther. 2020;13:6351-9.
15. Zhou C, Zhao X, Duan S. The role of miR-543 in human cancerous and noncancerous diseases. J Cell Physiol. 2020.
16. Otoukesh B, Abbasi M, Gorgani HO, Farahini H, Moghtadaei M, Boddouhi B, et al. MicroRNAs signatures, bioinformatics analysis of miRNAs, miRNA mimics and antagonists, and miRNA therapeutics in osteosarcoma. Cancer Cell Int. 2020;20:254.
17. Rzepiel A, Kutszegi N, Gezsi A, Sagi JC, Egyed B, Peter G, et al. Circulating microRNAs as minimal residual disease biomarkers in childhood acute lymphoblastic leukemia. J Transl Med. 2019;17(1):372.
18. Barcelo M, Castells M, Perez-Riba M, Bassas L, Vigues F, Larriba S. Seminal plasma microRNAs improve diagnosis/prognosis of prostate cancer in men with moderately altered prostate-specific antigen. Am J Transl Res. 2020;12(5):2041-51.

19. Feng L, Ma J, Ji H, Liu Y, Hu W. miR-330-5p suppresses glioblastoma cell proliferation and invasiveness through targeting ITGA5. Biosci Rep. 2017;37(3).
20. Su BB, Zhou SW, Gan CB, Zhang XN. MiR-330-5p regulates tyrosinase and PDIA3 expression and suppresses cell proliferation and invasion in cutaneous malignant melanoma. J Surg Res. 2016;203(2):434-40.
21. Trehoux S, Lahdaoui F, Delpu Y, Renaud F, Leteurtre E, Torrisani J, et al. Micro-RNAs miR-29a and miR-330-5p function as tumor suppressors by targeting the MUC1 mucin in pancreatic cancer cells. Biochim Biophys Acta. 2015;1853(10 Pt A):2392-403.
22. Wang R, Dong HX, Zeng J, Pan J, Jin XY. LncRNA DGCR5 contributes to CSC-like properties via modulating miR-330-5p/CD44 in NSCLC. J Cell Physiol. 2018;233(9):7447-56.
23. Fu X, Zhang L, Dan L, Wang K, Xu Y. LncRNA EWSAT1 promotes ovarian cancer progression through targeting miR-330-5p expression. Am J Transl Res. 2017;9(9):4094-103.
24. Gong D, Feng PC, Ke XF, Kuang HL, Pan LL, Ye Q, et al. Silencing Long Non-coding RNA LINC01224 Inhibits Hepatocellular Carcinoma Progression via MicroRNA-330-5p-Induced Inhibition of CHEK1. Mol Ther Nucleic Acids. 2020;19:482-97.
25. Yu LX, Zhang BL, Yang Y, Wang MC, Lei GL, Gao Y, et al. Exosomal microRNAs as potential biomarkers for cancer cell migration and prognosis in hepatocellular carcinoma patient-derived cell models. Oncol Rep. 2019;41(1):257-69.
26. Al-Abdulla R, Lozano E, Macias RIR, Monte MJ, Briz O, O'Rourke CJ, et al. Epigenetic events involved in organic cation transporter 1-dependent impaired response of hepatocellular carcinoma to sorafenib. Br J Pharmacol. 2019;176(6):787-800.
27. Xiao S, Yang M, Yang H, Chang R, Fang F, Yang L. miR-330-5p targets SPRY2 to promote hepatocellular carcinoma progression via MAPK/ERK signaling. Oncogenesis. 2018;7(11):90.
28. Hu X, Feng Y, Sun L, Qu L, Sun C. Roles of microRNA-330 and Its Target Gene ING4 in the Development of Aggressive Phenotype in Hepatocellular Carcinoma Cells. Dig Dis Sci. 2017;62(3):715-22.
29. Gao J, Yin X, Yu X, Dai C, Zhou F. Long noncoding RNA LINC00488 functions as a ceRNA to regulate hepatocellular carcinoma cell growth and angiogenesis through miR-330-5. Dig Liver Dis. 2019;51(7):1050-9.
30. Chen G, Umelo IA, Lv S, Teugels E, Fostier K, Kronenberger P, et al. miR-146a inhibits cell growth, cell migration and induces apoptosis in non-small cell lung cancer cells. PLoS One. 2013;8(3):e60317.
31. Rong M, He R, Dang Y, Chen G. Expression and clinicopathological significance of miR-146a in hepatocellular carcinoma tissues. Ups J Med Sci. 2014;119(1):19-24.
32. He RQ, Yang X, Liang L, Chen G, Ma J. MicroRNA-124-3p expression and its prospective functional pathways in hepatocellular carcinoma: A quantitative polymerase chain reaction, gene expression omnibus and bioinformatics study. Oncol Lett. 2018;15(4):5517-32.
33. Clough E, Barrett T. The Gene Expression Omnibus Database. Methods Mol Biol. 2016;1418:93-110.

34. Athar A, Fullgrabe A, George N, Iqbal H, Huerta L, Ali A, et al. ArrayExpress update - from bulk to single-cell expression data. Nucleic Acids Res. 2019;47(D1):D711-D5.
35. Leinonen R, Sugawara H, Shumway M, International Nucleotide Sequence Database C. The sequence read archive. Nucleic Acids Res. 2011;39(Database issue):D19-21.
36. Xie ZC, Li TT, Gan BL, Gao X, Gao L, Chen G, et al. Investigation of miR-136-5p key target genes and pathways in lung squamous cell cancer based on TCGA database and bioinformatics analysis. Pathol Res Pract. 2018;214(5):644-54.
37. Gao L, Zhang LJ, Li SH, Wei LL, Luo B, He RQ, et al. Role of miR-452-5p in the tumorigenesis of prostate cancer: A study based on the Cancer Genome Atl(TCGA), Gene Expression Omnibus (GEO), and bioinformatics analysis. Pathol Res Pract. 2018;214(5):732-49.
38. Dweep H, Gretz N. miRWalk2.0: a comprehensive atlas of microRNA-target interactions. Nat Methods. 2015;12(8):697.
39. Szklarczyk D, Gable AL, Lyon D, Junge A, Wyder S, Huerta-Cepas J, et al. STRING v11: protein-protein association networks with increased coverage, supporting functional discovery in genome-wide experimental datasets. Nucleic Acids Res. 2019;47(D1):D607-D13.
40. Yang X, Mo W, Fang Y, Wei G, Wei M, Dang Y, et al. Up-regulation of Polo-like Kinase 1 in nasopharyngeal carcinoma tissues: a comprehensive investigation based on RNA-sequencing, gene chips, and in-house tissue arrays. Am J Transl Res. 2018;10(12):3924-40.
41. Wei DM, Jiang MT, Lin P, Yang H, Dang YW, Yu Q, et al. Potential ceRNA networks involved in autophagy suppression of pancreatic cancer caused by chloroquine diphosphate: A study based on differentiallyexpressed circRNAs, lncRNAs, miRNAs and mRNAs. Int J Oncol. 2019;54(2):600-26.
42. Xiong DD, Dang YW, Lin P, Wen DY, He RQ, Luo DZ, et al. A circRNA-miRNA-mRNA network identification for exploring underlying pathogenesis and therapy strategy of hepatocellular carcinoma. J Transl Med. 2018;16(1):220.
43. Wen DY, Lin P, Liang HW, Yang X, Li HY, He Y, et al. Up-regulation of CTD-2547G23.4 in hepatocellular carcinoma tissues and its prospective molecular regulatory mechanism: a novel qRT-PCR and bioinformatics analysis study. Cancer Cell Int. 2018;18:74.
44. Pavlova NN, Thompson CB. The Emerging Hallmarks of Cancer Metabolism. Cell Metab. 2016;23(1):27-47.
45. DeBerardinis RJ, Mancuso A, Daikhin E, Nissim I, Yudkoff M, Wehrli S, et al. Beyond aerobic glycolysis: transformed cells can engage in glutamine metabolism that exceeds the requirement for protein and nucleotide synthesis. Proc Natl Acad Sci U S A. 2007;104(49):19345-50.
46. Weinberg F, Hamanaka R, Wheaton WW, Weinberg S, Joseph J, Lopez M, et al. Mitochondrial metabolism and ROS generation are essential for Kras-mediated tumorigenicity. Proc Natl Acad Sci U S A. 2010;107(19):8788-93.
47. Plaitakis A, Kalef-Ezra E, Kotzamani D, Zaganas I, Spanaki C. The Glutamate Dehydrogenase Pathway and Its Roles in Cell and Tissue Biology in Health and Disease. Biology (Basel). 2017;6(1).

48. Glazer RI, Vogel CL, Patel IR, Anthony PP. Glutamate dehydrogenase activity related to histopathological grade of hepatocellular carcinoma in man. Cancer Res. 1974;34(11):2975-8.
49. Hensley CT, Wasti AT, DeBerardinis RJ. Glutamine and cancer: cell biology, physiology, and clinical opportunities. J Clin Invest. 2013;123(9):3678-84.
50. Coloff JL, Murphy JP, Braun CR, Harris IS, Shelton LM, Kami K, et al. Differential Glutamate Metabolism in Proliferating and Quiescent Mammary Epithelial Cells. Cell Metab. 2016;23(5):867-80.
51. Nwosu ZC, Battello N, Rothley M, Pioronska W, Sitek B, Ebert MP, et al. Liver cancer cell lines distinctly mimic the metabolic gene expression pattern of the corresponding human tumours. J Exp Clin Cancer Res. 2018;37(1):211.
52. Mates JM, Segura JA, Martin-Rufian M, Campos-Sandoval JA, Alonso FJ, Marquez J. Glutaminase isoenzymes as key regulators in metabolic and oxidative stress against cancer. Curr Mol Med. 2013;13(4):514-34.
53. Chen SS, Yu KK, Ling QX, Huang C, Li N, Zheng JM, et al. The combination of three molecular markers can be a valuable predictive tool for the prognosis of hepatocellular carcinoma patients. Sci Rep. 2016;6:24582.

Tables

Table 1

Dataset	Author	Year	Country	Sample type	Experiment type
E-MTAB-4170	Masanori Nojima	2014	Japan	tissue	microRNA profiling by array
GSE104251	Wang Y	2018	China	serum exosomal	Non-coding RNA profiling by high throughput sequencing
GSE108724	Zhu HR	2018	China	tissue	Non-coding RNA profiling by array
GSE112264	Urabe F	2018	Japan	serum	Non-coding RNA profiling by array
GSE115016	Ye G	2018	China	tissue	Non-coding RNA profiling by array
GSE21362	Sato F	2011	Japan	tissue	Non-coding RNA profiling by array
GSE22058	Burchard J	2010	USA	tissue	Non-coding RNA profiling by array
GSE36915	Yun-Shien Lee	2013	Taiwan	tissue	Non-coding RNA profiling by array
GSE39678	Kim J	2012	South Korea	tissue	Non-coding RNA profiling by array
GSE40744	Diaz G	2013	USA	tissue	Non-coding RNA profiling by array
GSE41874	Morita K	2013	Japan	tissue	Non-coding RNA profiling by array
GSE51429	Perell K	2013	Denmark	tissue	Expression profiling by RT-qPCR
GSE53992	Plieskatt JL	2014	USA	tissue	Non-coding RNA profiling by array
GSE54751	Shen J	2014	USA	tissue	Expression profiling by RT-qPCR
GSE57555	Taguchi Y	2015	Japan	tissue	Non-coding RNA profiling by array
GSE59856	Kojima M	2014	Japan	serum	Non-coding RNA profiling by array
GSE63046	Jazdzewski K	2014	Poland	tissue	Non-coding RNA profiling by high throughput sequencing
GSE64632	Peng H	2015	Poland	tissue	Non-coding RNA profiling by array
GSE6857	Budhu A	2007	USA	tissue	Non-coding RNA profiling by array
GSE69580	Hung C	2015	Taiwan	tissue	Non-coding RNA profiling by array
GSE74618	Villanueva A	2016	Spain	tissue	Non-coding RNA profiling by array
GSE98269	Xie Z	2017	China	tissue	Non-coding RNA profiling by array
GSE98406	Kelley KA	2017	USA	tissue	Non-coding RNA profiling by array

Characteristics of microarray and RNA-seq datasets included in the study of miR-330-5p.

Table 2

clinical parameters	n	mean ± SD		P
Gender				
male	279	3.7397	0.96217	0.961
female	141	3.7349	0.98041	
Age				
≤60	195	3.8892	1.03242	0.002*
60	224	3.6022	0.88744	
grade				
G1-G2	261	3.6204	0.9299	0.001*
G3-G4	152	3.9483	1.01471	
Stage				
I-II	287	3.6763	0.91312	0.029*
III-IV	102	3.9207	1.11257	
T				
T1	201	3.6304	0.88442	0.024*
T2-T4	216	3.8444	1.03311	
N				
N0	284	3.7631	0.99708	0.754
N1	5	3.6222	0.83135	
M				
M0	300	3.7696	1.003	0.862
M1	5	3.691	0.88819	
Alcohol addiction				
Yes	125	3.7519	0.98552	0.572
No	109	3.678	1.01126	
HBV infection				
Yes	90	3.7572	0.90771	0.565
No	109	3.678	1.01126	
HCV infection				

Yes	38	3.908	0.81183	0.218
No	110	3.6841	1.00866	
albumin value				
low	159	3.8808	1.05834	0.018*
Normal	250	3.6476	0.89835	

The correlation between clinicopathological variables and miR-330-5p expression in HCC from TCGA.
*P<0.05

Table 3

clinical parameters	n	mean±SD		P
Age				
≤60	15	2.7564	1.27772	0.038*
60	11	1.5432	1.54149	
Gender				
male	20	2.2902	1.4937	0.776
female	6	2.086	1.6355	
Metastasis				
M0	6	0.3527	0.66802	<0.001*
M1	20	2.8102	1.16648	
Nodes				
single	11	1.6722	1.55538	0.096
multiple	15	2.6617	1.35101	
Tumor diameter				
<5cm	7	2.4391	0.9529	0.616
>=5cm	19	2.1709	1.66904	
Vascular invasion				
NO	15	1.8644	1.48311	0.134
YES	11	2.7595	1.41699	
Tumor thrombus				
NO	16	1.7802	1.52354	0.043*
YES	10	2.9837	1.16559	
Grade				
I-II	21	2.1439	1.4276	0.500
III-IV	5	2.6597	1.87903	
AFP				
negative	10	2.0917	1.44279	0.576
positive	13	2.4639	1.63681	
nm23 related				

-	2	1.1427	0.34647	0.288
+	24	2.3348	1.52108	
p53 related				
-	6	2.5894	1.76683	0.529
+	20	2.1392	1.4403	
p21 related				
-	13	2.6377	1.36508	0.184
+	13	1.8485	1.56919	
VEGF related				
-	3	1.9777	1.23078	0.751
+	23	2.2777	1.54758	
ki67 related				
-	9	1.9877	1.71174	0.538
+	17	2.3783	1.4058	

The correlation between clinicopathological variables and miR-330-5p expression in HCC from in house RT-qPCR. *P<0.05.

Table 4

Category	Term	Count	P Value
GOTERM_BP_DIRECT	GO:0042493~response to drug	23	2.90E-05
GOTERM_BP_DIRECT	GO:0008203~cholesterol metabolic process	10	8.54E-05
GOTERM_BP_DIRECT	GO:0010628~positive regulation of gene expression	19	2.90E-04
GOTERM_BP_DIRECT	GO:0043410~positive regulation of MAPK cascade	10	3.32E-04
GOTERM_BP_DIRECT	GO:0006520~cellular amino acid metabolic process	7	6.65E-04
GOTERM_BP_DIRECT	GO:0006954~inflammatory response	23	6.83E-04
GOTERM_BP_DIRECT	GO:0055114~oxidation-reduction process	31	7.56E-04
GOTERM_BP_DIRECT	GO:0043401~steroid hormone mediated signaling pathway	8	8.29E-04
GOTERM_BP_DIRECT	GO:0007566~embryo implantation	7	8.68E-04
GOTERM_BP_DIRECT	GO:0030336~negative regulation of cell migration	10	0.001073
GOTERM_CC_DIRECT	GO:0070062~extracellular exosome	116	3.57E-07
GOTERM_CC_DIRECT	GO:0005887~integral component of plasma membrane	66	6.00E-06
GOTERM_CC_DIRECT	GO:0009897~external side of plasma membrane	18	4.79E-05
GOTERM_CC_DIRECT	GO:0005759~mitochondrial matrix	23	5.46E-05
GOTERM_CC_DIRECT	GO:0005886~plasma membrane	144	9.64E-05
GOTERM_CC_DIRECT	GO:0005615~extracellular space	54	0.001885
GOTERM_CC_DIRECT	GO:0030667~secretory granule membrane	5	0.001947
GOTERM_CC_DIRECT	GO:0005829~cytosol	112	0.002731
GOTERM_CC_DIRECT	GO:0016021~integral component of membrane	164	0.002769
GOTERM_CC_DIRECT	GO:0009986~cell surface	26	0.004639
GOTERM_MF_DIRECT	GO:0008092~cytoskeletal protein binding	8	2.83E-04
GOTERM_MF_DIRECT	GO:0003707~steroid hormone receptor activity	8	7.41E-04
GOTERM_MF_DIRECT	GO:0008134~transcription factor binding	19	7.47E-04
GOTERM_MF_DIRECT	GO:0016491~oxidoreductase activity	15	0.001105
GOTERM_MF_DIRECT	GO:0005539~glycosaminoglycan binding	5	0.00119

GOTERM_MF_DIRECT	GO:0050660~flavin adenine dinucleotide binding	8	0.00165
GOTERM_MF_DIRECT	GO:0005515~protein binding	269	0.002005
GOTERM_MF_DIRECT	GO:0042803~protein homodimerization activity	34	0.002792
GOTERM_MF_DIRECT	GO:0009055~electron carrier activity	9	0.002987
GOTERM_MF_DIRECT	GO:0030170~pyridoxal phosphate binding	7	0.004258

Functional annotation of the gene ontology (GO) of overlapping genes. Note: BP, biological process; CC, cellular component; MF, molecular function.

Table 5

Category	Term	Count	P Value
KEGG_PATHWAY	hsa00250:Alanine, aspartate and glutamate metabolism	8	1.77E-04
KEGG_PATHWAY	hsa01100:Metabolic pathways	64	6.48E-04
KEGG_PATHWAY	hsa05200:Pathways in cancer	27	0.001305
KEGG_PATHWAY	hsa00260:Glycine, serine and threonine metabolism	7	0.002192
KEGG_PATHWAY	hsa00380:Tryptophan metabolism	7	0.002504
KEGG_PATHWAY	hsa00410:beta-Alanine metabolism	6	0.004152
KEGG_PATHWAY	hsa00280:Valine, leucine and isoleucine degradation	7	0.005709
KEGG_PATHWAY	hsa00340:Histidine metabolism	5	0.00663
KEGG_PATHWAY	hsa04610:Complement and coagulation cascades	8	0.010305
KEGG_PATHWAY	hsa05215:Prostate cancer	9	0.011891

Functional annotation of the KEGG pathway analysis of overlapping genes. Note: KEGG, Kyoto Encyclopedia of Genes and Genomes.

Figures

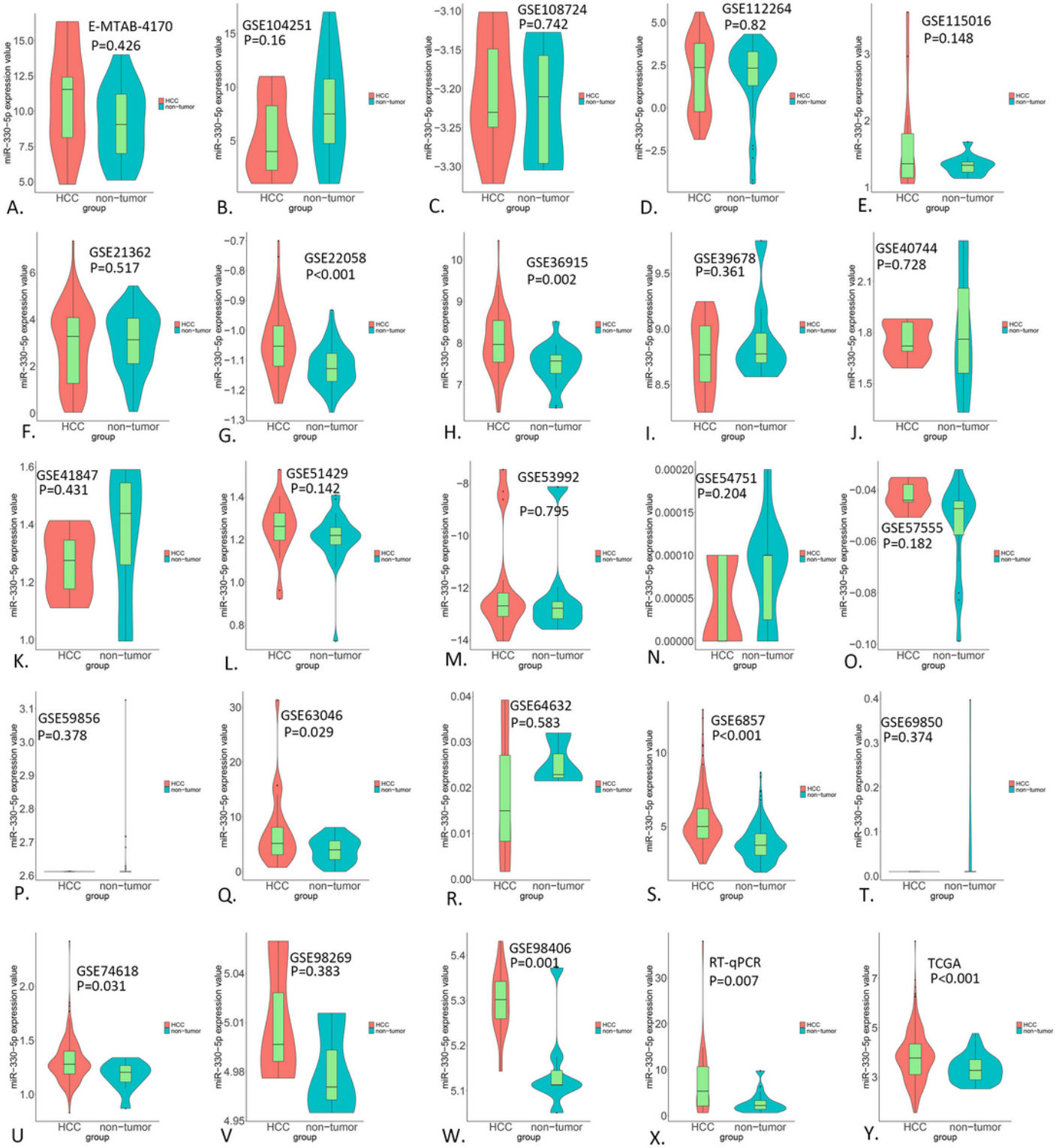

Figure 1

The expression of miR-330-5p in each study. The width of violin was reflected the samples enrichment degree and the box plot was reflected the mean value and quartile. (A)E-MTAB-4170. (B)GSE104251. (C)GSE108724. (D)GSE112264. (E)GSE115016. (F)GSE21362. (G)GSE22058. (H)GSE36915. (I)GSE39678. (J)GSE40744. (K)GSE41847. (L)GSE51429. (M)GSE53992. (N)GSE54751. (O)GSE57555.

(P)GSE59856. (Q)GSE63046. (R)GSE64632. (S)GSE6857. (T)GSE69580. (U)GSE74618. (V)GSE98269. (W)GSE98406. (X)RT-qPCR. (Y)TCGA.

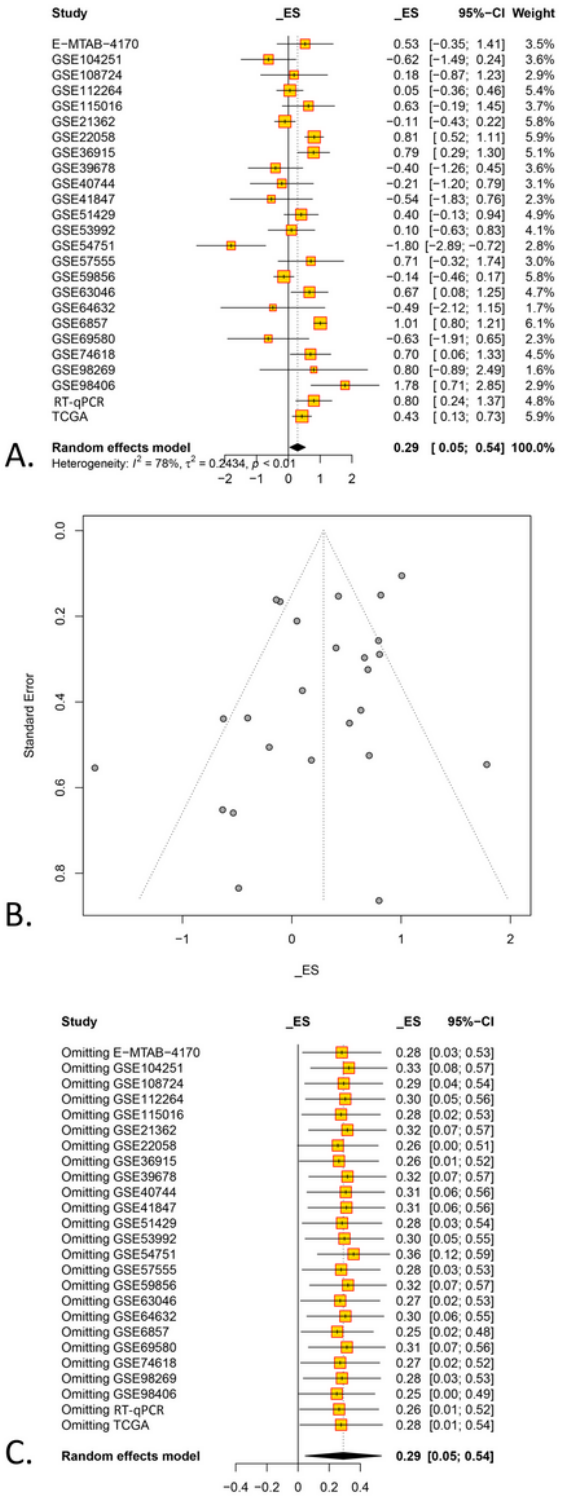

Figure 2

A meta-analysis analysis of miR-330-5p in HCC and non-tumor tissue. (A) Combined with a series of studies, the expression trend of miR-330-5p in HCC and non-tumor tissue was shown by forest plot. A

random effects model was used. (B) Funnel plot was drawn to estimate the publication bias. (C) Sensitivity analysis was performed to find out the high heterogeneity studies.

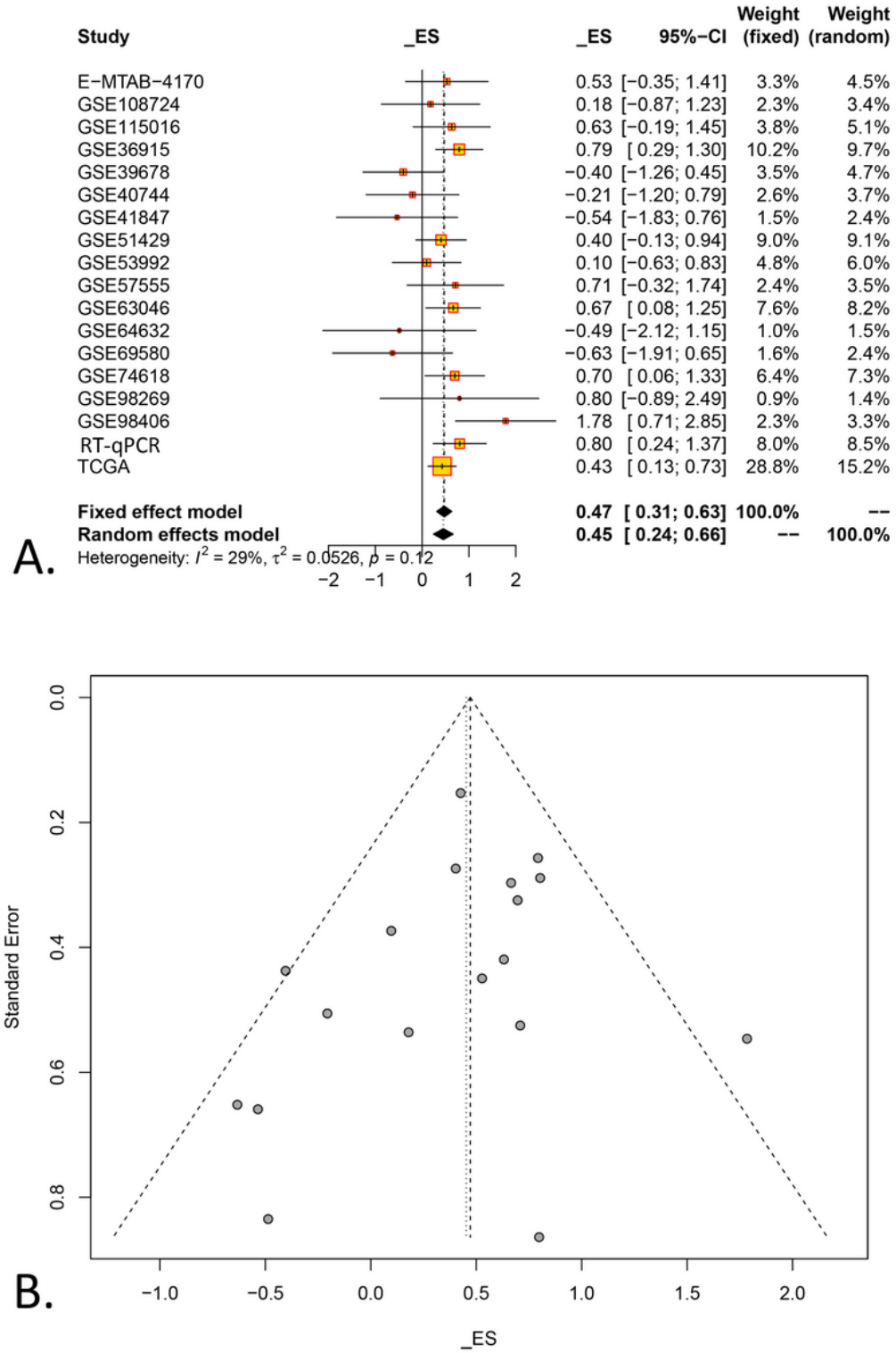

Figure 3

Further meta-analysis of integrative studies after excluding GSE21362. (A) A random effect model was used in the further analysis. (B) Funnel plot of included studies excluding GSE21362.

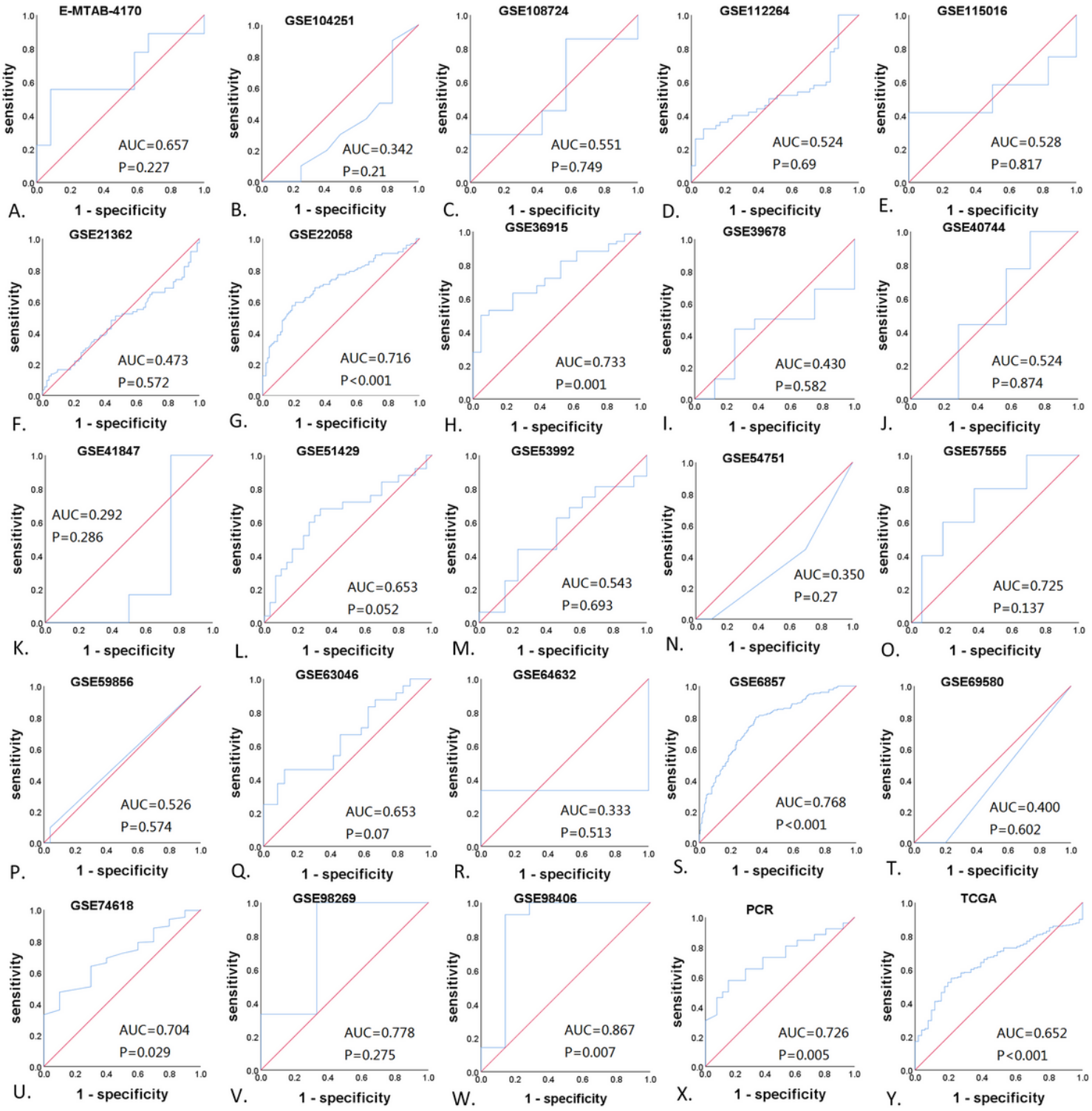

Figure 4

The roc curves were performed for each study. (A)E-MTAB-4170. (B)GSE104251. (C)GSE108724. (D)GSE112264. (E)GSE115016. (F)GSE21362. (G)GSE22058. (H)GSE36915. (I)GSE39678. (J)GSE40744. (K)GSE41847. (L)GSE51429. (M)GSE53992. (N)GSE54751. (O)GSE57555. (P)GSE59856. (Q)GSE63046. (R)GSE64632. (S)GSE6857. (T)GSE69580. (U)GSE74618. (V)GSE98269. (W)GSE98406. (X)RT-qPCR. (Y)TCGA.

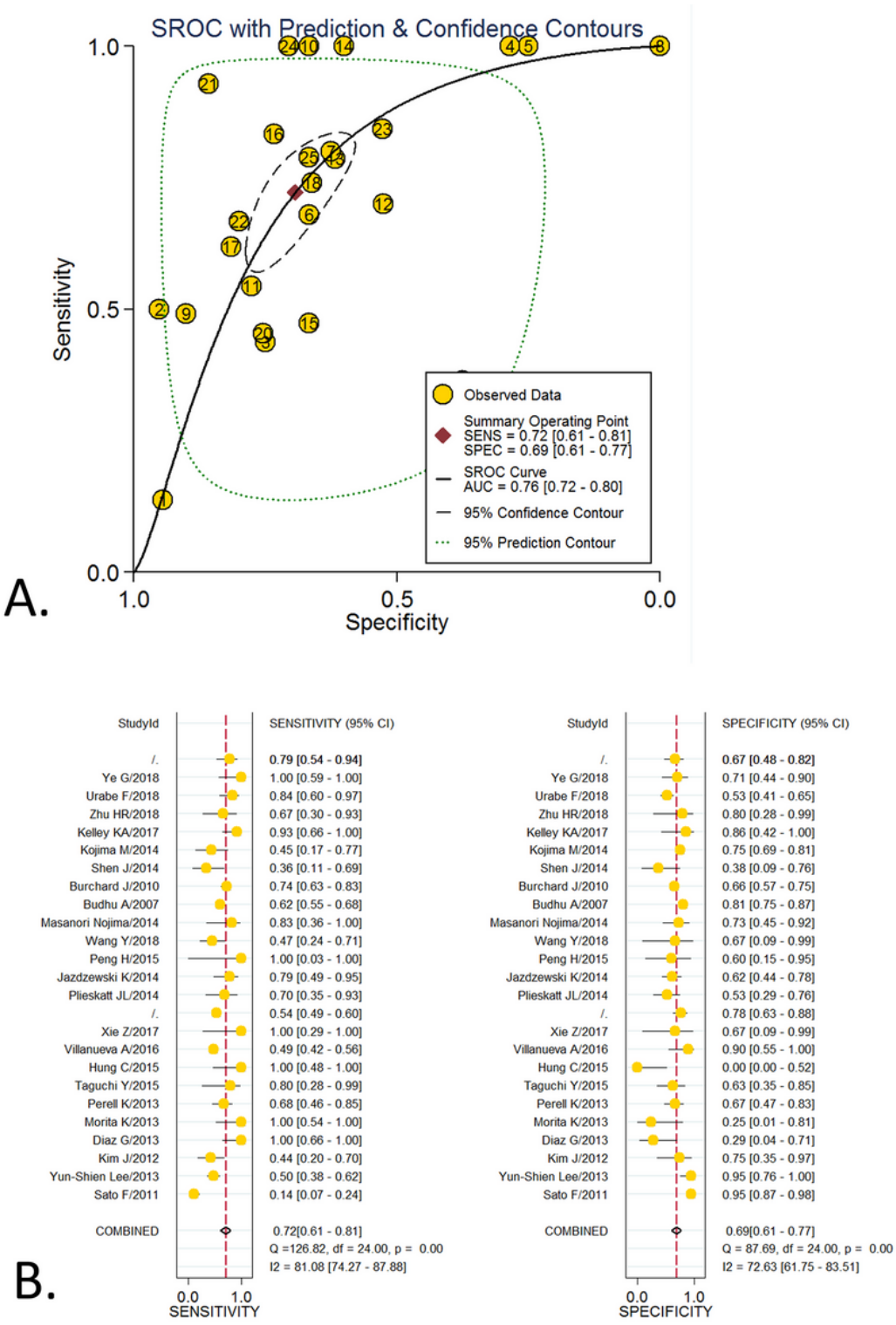

Figure 5

(A) SROC curves based on the integrative studies. (B) The sensitivity and specificity of SROC curve.

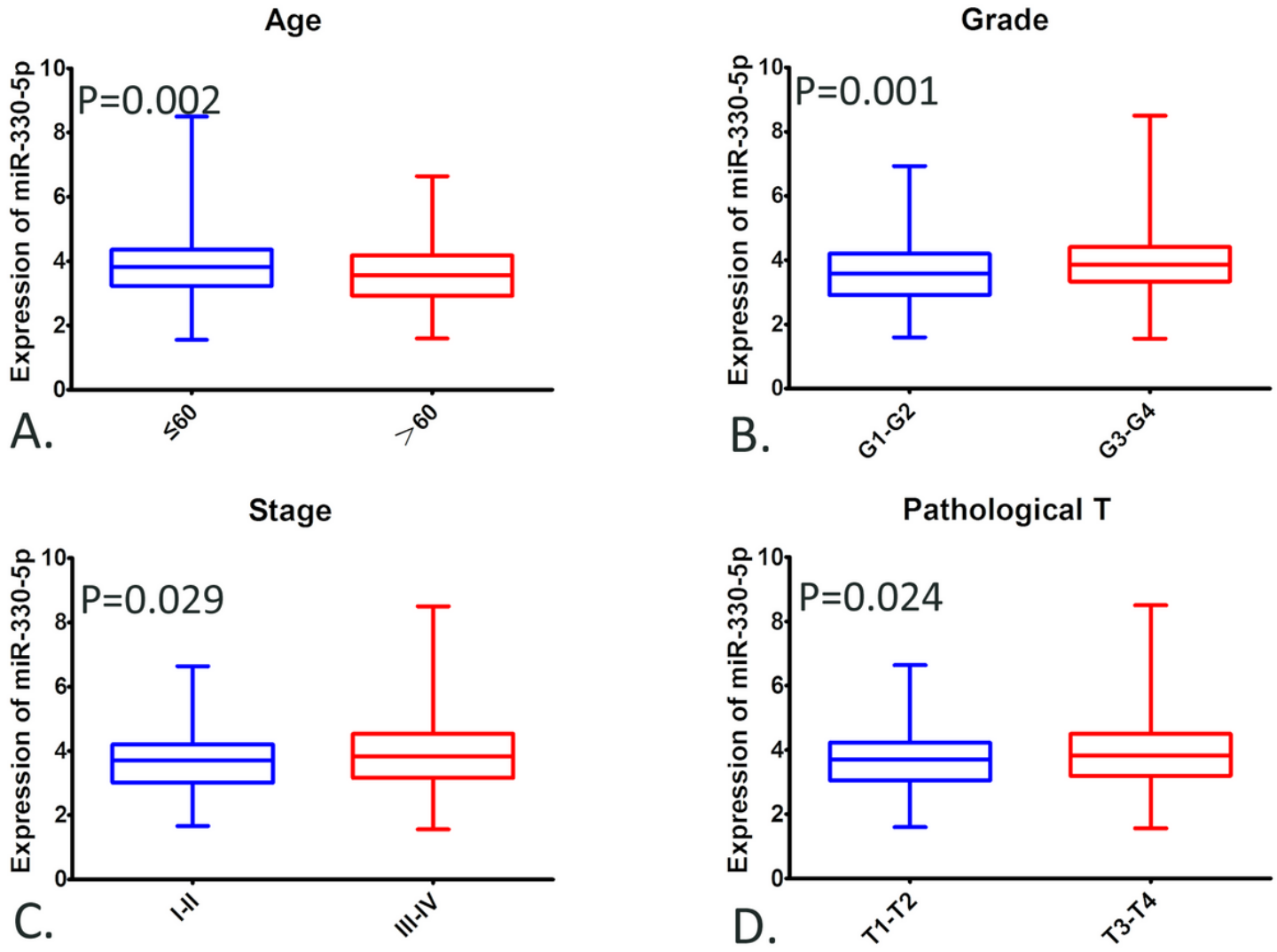

Figure 6

The expression level of miR-330-5p in different pathological parameter groups based on TCGA. (A)Age. (B) Grade. (C) Stage. (D) Pathological T.

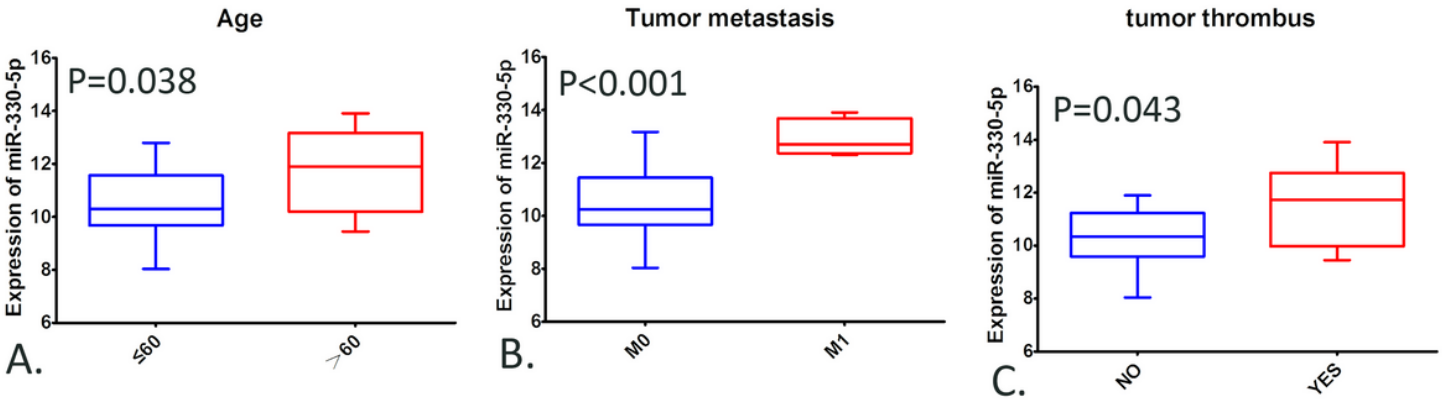

Figure 7

The expression level of miR-330-5p in different pathological parameter groups based on RT-qPCR. (A) Age. (B) Tumor metastasis. (C) Tumor thrombus.

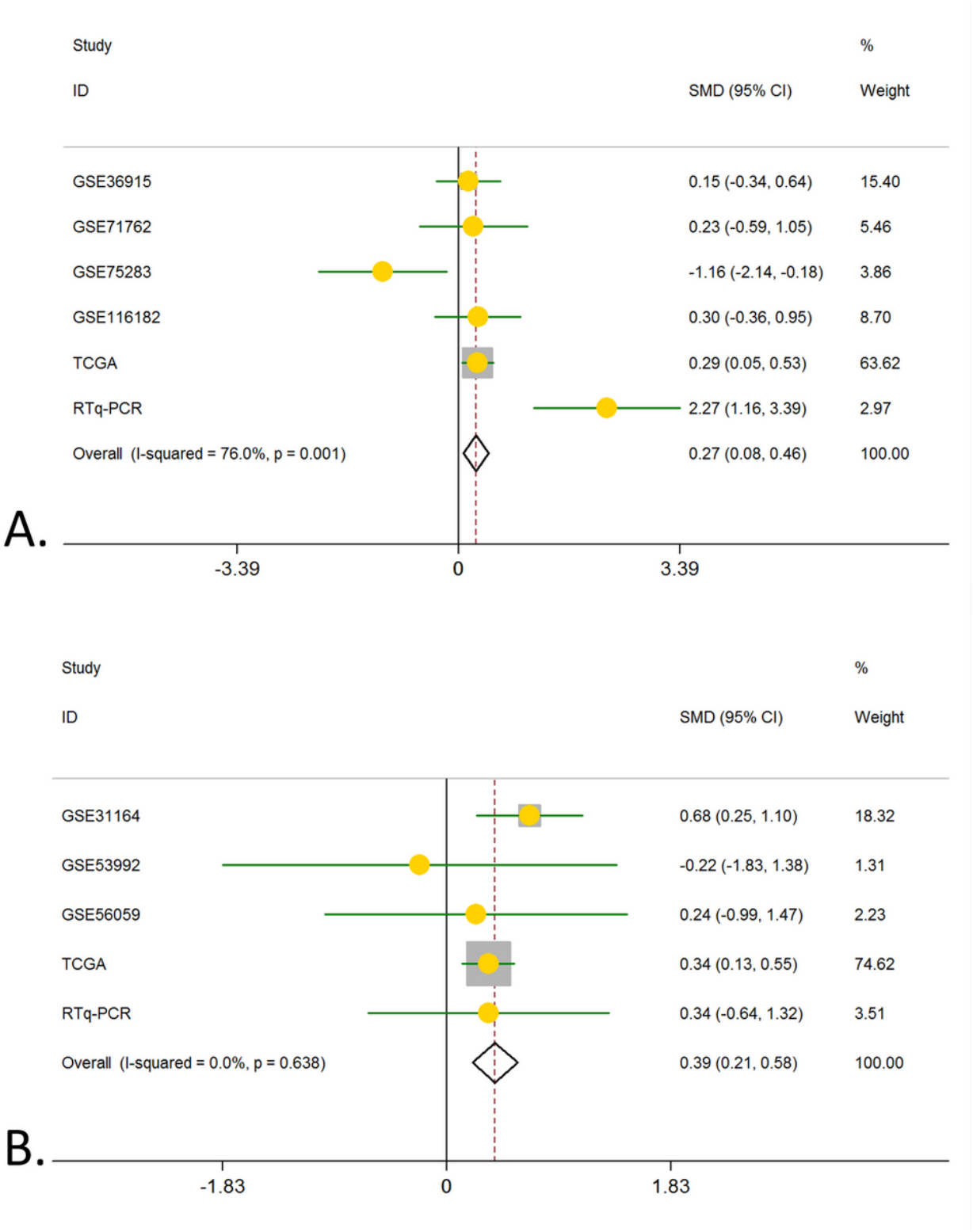

Figure 8

(A) A meta-analysis of miR-330-5p based on HCC progression parameters. (B) A meta-analysis of miR-330-5p based on HCC grade.

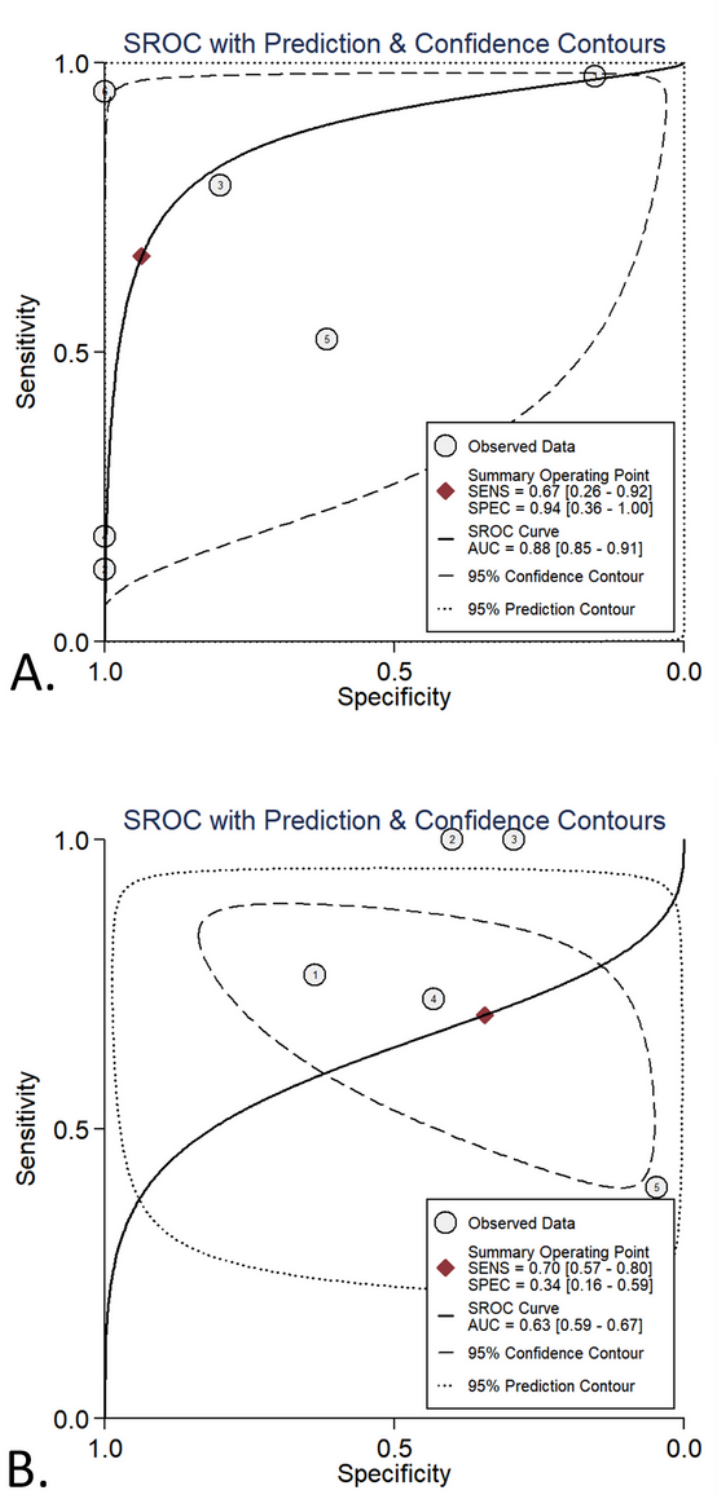

Figure 9

(A) SROC curves of stage group. (B) SROC curves of grade group.

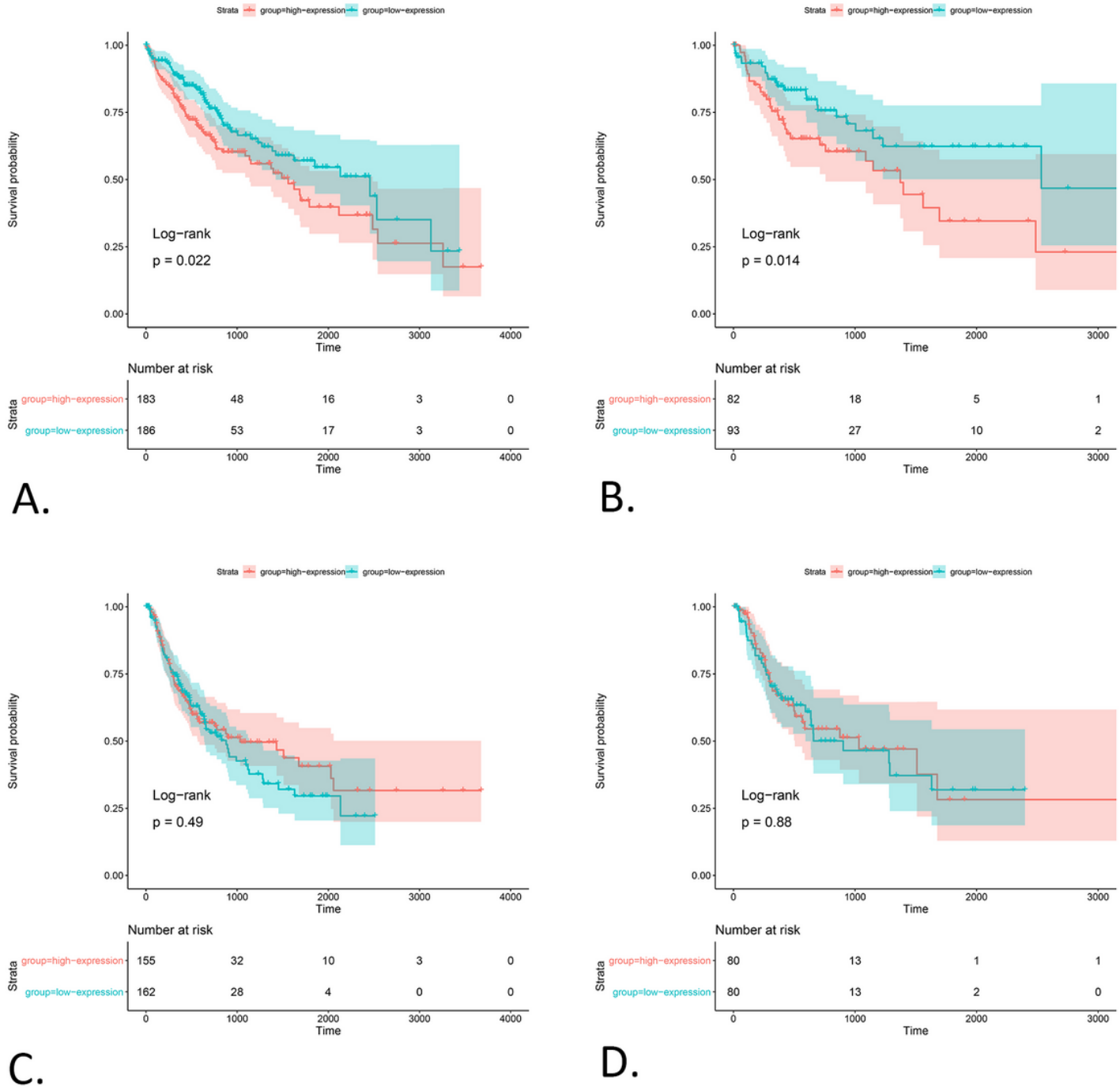

Figure 10

K-M plots of overall survival and relapse-free survival based on TCGA data. (A)The expression value of miR-330-5p was divided into high expression group and low expression group based on the mean value, and the prognosis was compared between the two groups in OS. (B) The expression value of miR-330-5p was divided into high expression group and low expression group based on the quartile, and the prognosis was compared between the two groups in OS. (C) The expression value of miR-330-5p was divided into high expression group and low expression group based on the mean value, and the prognosis

was compared between the two groups in RFS. (D) The expression value of miR-330-5p was divided into high expression group and low expression group based on the quartile, and the prognosis was compared between the two groups in RFS.

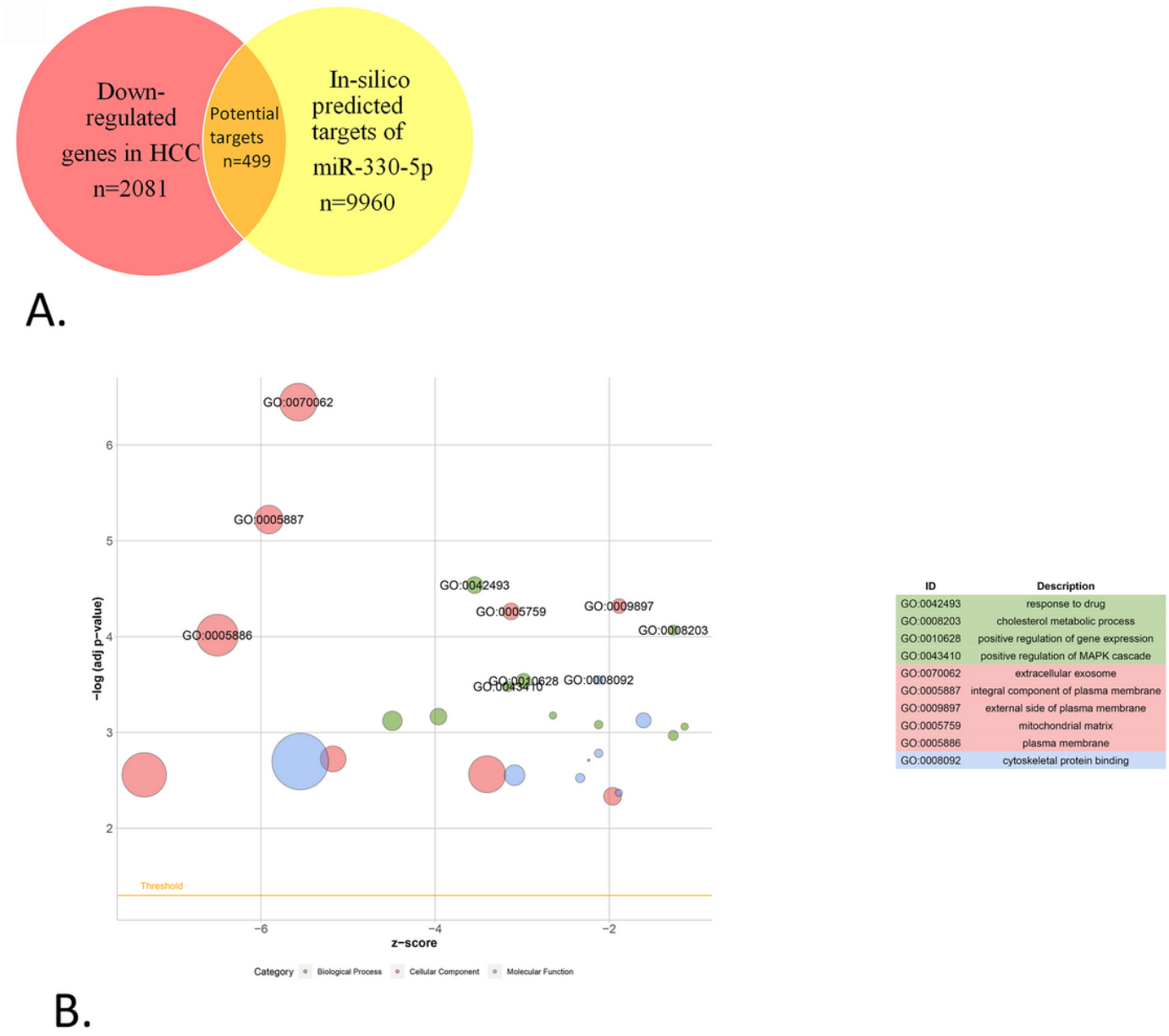

Figure 11

The overlapping genes and GO analysis. (A) The overlapping genes were screened between DEGs and the target genes of miR-330-5p. (B) Bubble plot was performed for GO analysis. Green bubbles were BP terms, red bubbles were CC terms and blue bubbles were MF terms. The size of bubble was associated with the gene counts.

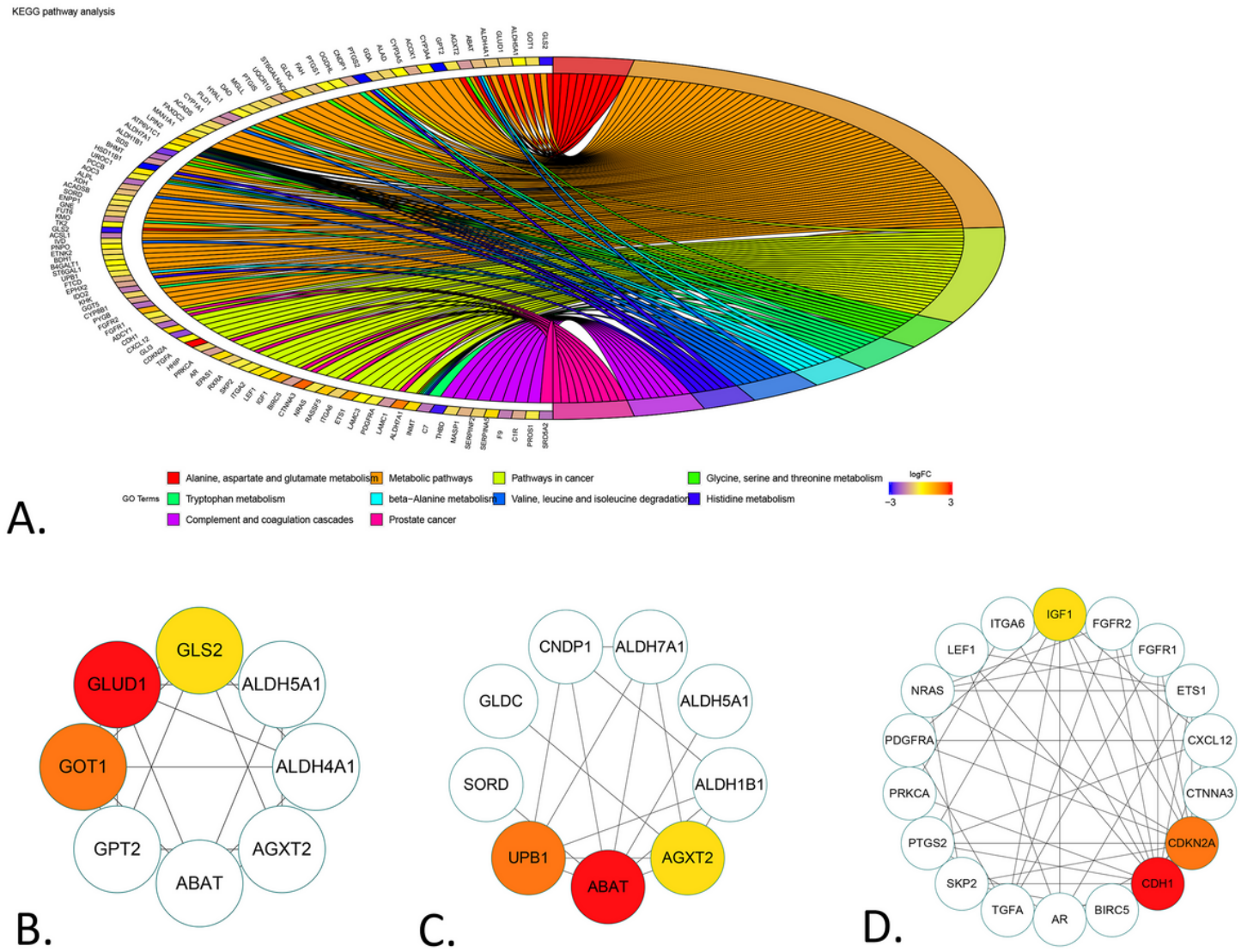

Figure 12

KEGG pathway analysis and PPI network were visualized. (A) Chord diagram was performed for KEGG pathways based on overlapping genes. (B-D) The genes with color were the hub genes in each PPI network, and the gene in red color was the most important gene.

Supplementary Files

This is a list of supplementary files associated with this preprint. Click to download.

- floatimage13.png